PHYSICAL REVIEW E **75**, 020401(R) (2007)

Anomalous collective dynamics in optically driven colloidal rings

Yael Roichman and David G. Grier
Department of Physics and Center for Soft Matter Research, New York University, New York, New York 10003, USA

George Zaslavsky
Department of Physics and Courant Institute, New York University, New York, New York 10003, USA

(Received 22 May 2006; revised manuscript received 21 December 2006; published 6 February 2007)

Three fluid-borne colloidal spheres circulating around a ringlike optical vortex trap have been predicted to undergo periodic collective motion due to their hydrodynamic coupling. In fact, the quenched disorder in an experimentally projected optical vortex drives a transition to a dynamical state characterized by power-law divergence of phase-space trajectories and collective fluctuations characterized by noninteger exponents. The observed relationship between scaling in the microscopic trajectories and macroscopic collective fluctuations is consistent with predictions for the onset of weak chaos within the experimentally accessible time window.

DOI: 10.1103/PhysRevE.75.020401 PACS number(s): 82.70.Dd, 05.45.Ac, 87.80.Cc

Three identical spheres slowly sedimenting through a viscous fluid in two or three dimensions generically tumble chaotically [1]. When the same spheres are driven steadily around a ring, by contrast, their motion is predicted to be purely periodic [2], with the reduction in dimensionality and the imposition of periodic boundary conditions [3] effectively eliminating the domain of chaotic dynamics. In this Rapid Communication, we demonstrate experimentally that quenched disorder can randomize this system's trajectory through phase space, replacing the periodic steady state with a power-law distribution of Poincaré recurrences. The hydrodynamically coupled spheres' collective motions also are characterized by power-law-distributed flights. The observed noninteger scaling in the microscopic and macroscopic degrees of freedom and the relationship between the extracted scaling exponents are consistent with fractional or *strange* kinetics [4] in a system exhibiting weak chaos.

Our system consists of colloidal polystyrene spheres 1.51 μm in diameter (Polysciences, Lot No. 526826) dispersed in a layer of water 40 μm thick between a glass microscope slide and a coverslip. Three of these spheres are confined to a horizontal ring by a single-beam optical trap known as an optical vortex [5]. An optical vortex is formed by focusing a helical mode of light [6] with a high-numerical-aperture lens. The helical mode's wave fronts form an ℓ-fold helix, where ℓ is an integer winding number known as the topological charge. The associated ℓ-fold axial screw dislocation manifests itself in perfect destructive interference along the optical axis, so that the beam focuses onto a ring of light whose radius is proportional to ℓ [7]. Polarizable particles are drawn up intensity gradients to the bright ring, where they are trapped. Each photon in a helical beam, moreover, carries $\ell\hbar$ orbital angular momentum that can be transferred to trapped objects [8]. This creates a constant torque that drives the particles around the ring.

Our samples are mounted on the stage of a Nikon TE-2000U inverted optical microscope, whose objective lens [100× numerical aperture (NA) 1.4 oil immersion Plan-Apo] is used both to project an optical vortex and also to image the circulating spheres. We imprint helical phase profiles onto the wave fronts of a TEM_{00} beam (Coherent Verdi, $\lambda = 532$ nm) using a phase-only spatial light modulator (Hamamatsu X8267-16 PPM) in the holographic optical trapping configuration [9,10].

Figure 1(a) shows an optical vortex with $\ell = 80$ whose image was obtained by placing a front-surface mirror in the microscope's focal plane and collecting the reflected light with the objective lens. The bright central spot is a conventional optical tweezer formed on the optical axis by the undiffracted portion of the laser beam. After adaptively correcting for residual aberrations in the optical train [9,11], the optical vortex is a nearly uniform ring of light with radius $R_\ell = 12$ μm. Figure 1(b) shows three colloidal spheres trapped on the ring at an applied laser power of 2.5 W. Under these conditions, the particles circulate once around the ring in $T = 1.2$ s. We track the spheres' angular positions $\theta_1(t)$, $\theta_2(t)$, and $\theta_3(t)$ by recording the video stream at 30 frames per second on a Pioneer 520H-S digital video recorder (DVR) with a NEC TI-324AII monochrome video camera and extracting their instantaneous positions at 20 nm resolution using digital video analysis [12].

The optical vortex's circumferential intensity profile, plotted in Fig. 1(c), varies by about 20% from the mean. These

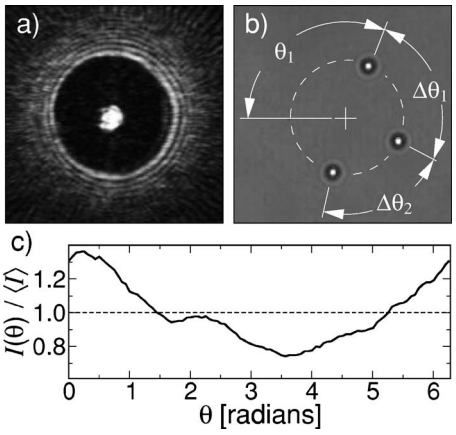

FIG. 1. Optically driven colloidal ring. (a) Projected intensity pattern for an optical vortex with $\ell = 80$. (b) Video microscope image of three colloidal silica spheres trapped on the optical vortex. (c) Measured intensity variations around the optical vortex's circumference.

intensity variations establish an effective potential energy landscape that the circulating particles revisit with each transit [13]. No minima are deep enough to trap a particle. Instead, fluctuations in a single particle's speed indicate root-mean-squared potential energy variations smaller than 5% of the mean.

A circulating sphere entrains flows in the surrounding fluid that exert forces on neighboring spheres. Treating the hydrodynamic coupling in the stokeslet approximation [14] reveals that the symmetric configuration of equally spaced particles is linearly unstable against a dynamical state comprised of a closely spaced pair of spheres and a singleton. The pair outpaces the singleton to form a transient three-particle cluster whose leading pair rushes ahead, leaving the last sphere behind [2]. This periodic state ought to be observed almost exclusively. Images such as Fig. 1(b), however, show the particles in the nominally unstable state.

This qualitative discrepancy with theory presumably results from forces in the experimental system not considered in the analytical model. Particles circulating around an optical vortex are affected by three factors: thermal forces, the optical vortex's fixed potential energy landscape, and the spheres' hydrodynamic interactions. Their relative importance can be inferred by comparing the measured [12] free-particle self-diffusion coefficient $D_0=0.19\pm0.02\ \mu\mathrm{m}^2/\mathrm{s}$ with that of a single sphere in the optical vortex [13], $D_d=1.0\pm0.2\ \mu\mathrm{m}^2/\mathrm{s}$, and with that of any one of the three spheres in Fig. 1(b), $D_{dc}=2.0\pm0.3\ \mu\mathrm{m}^2/\mathrm{s}$. In all three cases, the particle's mean-square positional fluctuations exhibit normal Einstein-Smoluchowsky scaling over the entire duration of the experiments [13].

We would not observe normal single-particle diffusion in the three-particle ring if interactions led to collective effects such as caging. Adding still more particles to the ring reduces their mean separation, increases crowding, and induces a crossover to single-file diffusion similar to that observed in related experiments on confined [15] and optically trapped colloid [16]. Unlike previous reports, the driving and disorder in our system allow for both subdiffusive and superdiffusive single-file motion, which will be discussed elsewhere. Anomalous three-particle dynamics in the present experiment instead reflects the evolution of correlations among the individual particles' trajectories.

A driven sphere's diffusion is strongly influenced by the optical vortex's potential energy landscape [13], with a single driven sphere's effective diffusivity D_d exceeding the free-particle value D_0 by a factor of 5. A single particle diffuses still more vigorously when it is hydrodynamically coupled to others on the ring, with $D_{dc}=2\ D_d=10D_0$. This further demonstrates that disorder-induced fluctuations are enhanced by interparticle interactions. Because hydrodynamic coupling alone would yield a periodic orbit [2], the aperiodic dynamics we observe must result from the disorder.

The optical vortex's potential energy landscape is fixed in both position and time. It acts as a periodic perturbation to the particles' trajectories because they revisit the same intensity variations with each cycle. Periodic perturbations are known to induce transitions to chaos [17,18] in a wide variety of Hamiltonian and non-Hamiltonian systems. Observed transitions between stable and unstable states in the optically driven colloidal ring might therefore signal the onset of chaos.

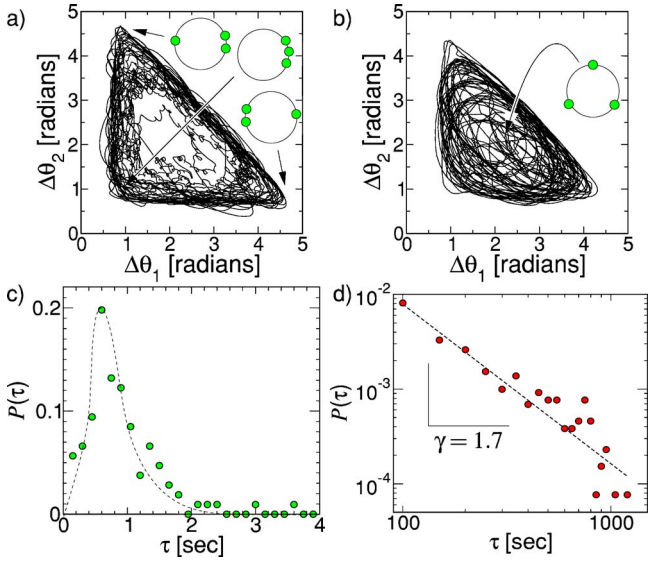

FIG. 2. (Color online) (a) Projection from the phase space reconstructed from particle tracks at $\ell=50$ and (b) $\ell=80$. (c) Recurrence time distribution for $\ell=50$. The curve is a guide to the eye suggesting a cycle period of 0.6 s. (d) Power-law recurrence time distribution for $\ell=80$.

To characterize the system's microscopic dynamics, we projected the trajectories onto the two-dimensional subspace of the six-dimensional phase space consisting of the independent angular separations $\Delta\theta_1(t)=\theta_2(t)-\theta_1(t)$ and $\Delta\theta_2(t)=\theta_3(t)-\theta_2(t)$. The results in Figs. 2(a) and 2(b) show continuous trajectories, each obtained over 2.5 h, for $\ell=50$ and $\ell=80$, respectively. The parametric traces were smoothed by box car averaging over ten mean circulation periods T to suppress details due to diffusion and disorder, and thus to provide a clearer picture of the system's intrinsic behavior.

Results for different topological charges differ qualitatively. The toroidal trace in Fig. 2(a) exhibits the predicted periodic orbit [2] with a characteristic cycle time of $\tau=0.6$ s. This exceeds the $T=0.3$ s required for an individual particle to circulate once around the ring. The dynamical state itself therefore rotates around the ring and is not phase locked to the landscape.

Increasing the topological charge from $\ell=50$ to $\ell=80$ increases R_ℓ from 8 μm to 12 μm, thereby separating the spheres and spreading the light over a larger circumference. The driving force on each particle decreases proportionately, as does the hydrodynamic coupling among particles. The landscape's disorder also weakens, but only proportionally to the decreased intensity. Increasing the topological charge therefore increases disorder's influence relative to hydrodynamic forces. Under these conditions, the spheres' trajectories make frequent and extended excursions away from the nominally stable periodic cycle into the region of phase space corresponding to the nominally unstable equilateral configuration.

We characterized both systems' microscopic dynamics by measuring the distribution $P(\tau)$ of Poincaré recurrence times

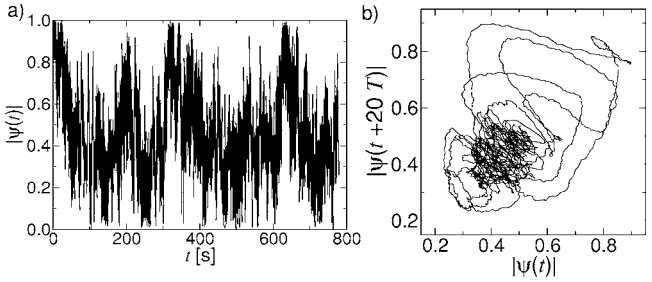

FIG. 3. (a) Evolution of the threefold bond-orientational order parameter. (b) Delay coordinate plot of $|\psi(t)|$ at lag $20T$.

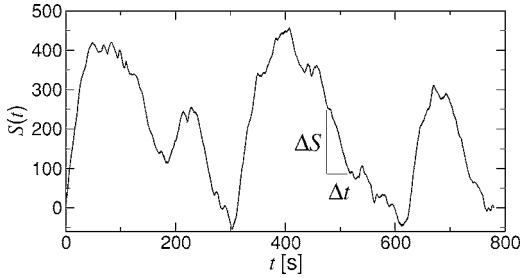

FIG. 4. Running sum $S(t)$ of the threefold bond-orientational order parameter, displaying a hierarchy of monotonic runs ΔS spanning a range of durations Δt.

τ required for a trajectory to revisit regions of phase space 0.5 rad on a side. Results for $\ell=50$ are plotted in Fig. 2(c) and are consistent with a simple cycle with a period of 0.6 s. Those for $\ell=80$, plotted in Fig. 2(d), are not periodic. Instead, $P(\tau)$ decays as a power law, with an exponent $\gamma=1.7\pm0.1$. This suggests a power-law divergence of trajectories in phase space, except over times τ shorter than T. This is a defining characteristic of weak chaos [19]. It is inconsistent with fully developed chaos whose trajectories should diverge exponentially.

The emergence of weak chaos driven by periodic perturbations has been inferred from measurements on nonlinear Alfvén waves in plasmas [20,21] and in low-dimensional wall flow of viscous fluids [22]. Noise-induced chaos of any kind is uncommon in strongly overdamped systems. Other known examples [23] rely on thermal forces to fully explore phase space. The present system, by contrast, relies on a combination of viscous damping and quenched disorder to access dynamically unfavorable states. Not any disordered landscape can induce chaos, moreover. As suggested in [18] and proved in [24], a periodic perturbation can open up a chaotic attractor near a stable limit cycle only if it possesses a broad frequency spectrum. Although experimental evidence alone is not sufficient to establish the existence of weak chaos in our system, notions from this formalism are useful for interpreting the emergence of random and phase-space-filling dynamics.

Having direct access to the microscopic degrees of freedom presents an unusual opportunity to see how dynamical randomness emerges in a driven dissipative system. To show this, we combine the three trajectories into the complex threefold bond-orientational order parameter,

$$\psi(t)=\frac{1}{3}\sum_{j=1}^{3}\exp[3i\theta_j(t)]. \tag{1}$$

This function's phase tracks the system's rotation about the optical axis and is useful for measuring the mean cycle period T. Its magnitude $|\psi(t)|$ reaches unity when the spheres are evenly spaced and drops to roughly one-third when a pair of spheres is diametrically opposite the third.

The trace of $|\psi(t)|$ in Fig. 3(a) is computed for the trajectory data in Fig. 2(b) and provides a macroscopic overview of the system's microscopic dynamics. As for other macroscopic descriptors, $\psi(t)$ can be used to reconstruct the underlying microscopic phase space. For example, Fig. 3(b) shows a Poincaré section at delay $20T$, which effectively fills the accessible part of the phase space. The periodic state concentrates the trajectory around $(1/3,1/3)$, while occasional excursions to the equilateral state fill out the pattern.

The order parameter's magnitude also confirms that the system switches intermittently between paired and equilateral states. To analyze the intermittent dynamics we use methods originally developed to interpret density fluctuations in tokamak plasmas [25].

Given measurements of $\psi(t)$ at N discrete times t_k, the running sum

$$S(t_n)=\sum_{k=1}^{n}|\psi(t_k)|-\frac{n}{N}[|\psi(t_N)|-|\psi(t_1)|] \tag{2}$$

emphasizes trends in $|\psi(t)|$, as shown in Fig. 4. Monotonic runs in $S(t)$ resemble *flights* in a system with fractional dynamics [4], an identification that is supported by the distribution functions plotted in Fig. 5. Not only does $|\psi(t)|$ display intermittency, but its two-state structure appears also to be scale invariant. The probability distributions for jump magnitudes and jump durations are both well described by power laws. The exponents $\alpha=-2.5\pm0.1$ and $\beta=-2.6\pm0.2$ for the magnitude and duration distributions, respectively, are consistent with each other, and both exceed 2. This is a signature of anomalous kinetics in the system's collective behavior [4]. Deviations from power-law scaling in $P_S(\Delta S)$ and $P_t(\Delta t)$ occur only for small flights, $\Delta S<3$, at short times, $\Delta t<10$ s, and thus a very small proportion of the measurement's dynamic range and duration. Consequently,

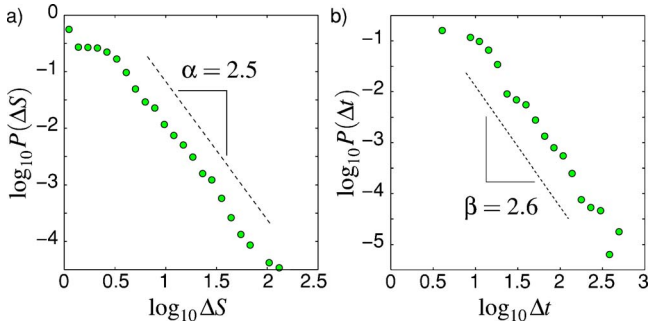

FIG. 5. (Color online) Scaling of the magnitude (a) and duration (b) distributions for runs in $S(t)$.

the system's Lyapunov exponents must be very small if not precisely zero.

Equality of α and β arises naturally in any system undergoing ballistic flights [19]. For the three colloidal spheres in the present model system, these flights take the form of random transitions between the equilateral and periodic dynamical states. Furthermore, log-periodic oscillations are evident when $S(t)$ is plotted on a logarithmic time scale. Such logarithmic periodicity arises for processes characterized by discrete scaling [19,26] and is evidence for hierarchical structure in the system's collective dynamics. If we assume that the scalings in $P(\tau)$ and $S(t)$ are consequences of the same dynamical process, the microscopic and macroscopic statistics are related by $P(\tau)d\tau = P_t(\Delta t)d\Delta t$ [4]. The associated scaling relation $\gamma = \alpha - 1$ is a characteristic of weak chaos and also is consistent with our data. Whether or not this indicates the existence of weak chaos and fractional dynamics in our system, this agreement points to a profound connection between microscopic degrees of freedom and nontrivial macroscopic fluctuations in an experimentally accessible driven dissipative system.

This work was supported by the National Science Foundation through Grant No. DMR-0451589. G.Z. was supported by ONR Grant No. N00014-02-1-0056. We would like to thank Pablo Jercog for inspiring discussions.

[1] I. M. Jánosi, T. Tél, D. E. Wolf, and J. A. C. Gallas, Phys. Rev. E **56**, 2858 (1997).
[2] M. Reichert and H. Stark, J. Phys.: Condens. Matter **16**, S4085 (2004).
[3] M. L. Ekiel-Jezewska and B. U. Felderhof, Phys. Fluids **17**, 093102 (2005).
[4] M. F. Shlesinger, G. M. Zaslavsky, and J. Klafter, Nature (London) **363**, 31 (1993).
[5] H. He, N. R. Heckenberg, and H. Rubinsztein-Dunlop, J. Mod. Opt. **42**, 217 (1995); K. T. Gahagan and G. A. Swartzlander, Opt. Lett. **21**, 827 (1996); N. B. Simpson, L. Allen, and M. J. Padgett, J. Mod. Opt. **43**, 2485 (1996).
[6] L. Allen, M. W. Beijersbergen, R. J. C. Spreeuw, and J. P. Woerdman, Phys. Rev. A **45**, 8185 (1992).
[7] J. E. Curtis and D. G. Grier, Phys. Rev. Lett. **90**, 133901 (2003); S. Sundbeck, I. Gruzberg, and D. G. Grier, Opt. Lett. **30**, 477 (2005).
[8] H. He, M. E. J. Friese, N. R. Heckenberg, and H. Rubinsztein-Dunlop, Phys. Rev. Lett. **75**, 826 (1995).
[9] M. Polin, K. Ladavac, S.-H. Lee, Y. Roichman, and D. G. Grier, Opt. Express **13**, 5831 (2005).
[10] E. R. Dufresne and D. G. Grier, Rev. Sci. Instrum. **69**, 1974 (1998); J. E. Curtis, B. A. Koss, and D. G. Grier, Opt. Commun. **207**, 169 (2002).
[11] Y. Roichman, A. S. Waldron, E. Gardel, and D. G. Grier, Appl. Opt. **45**, 3425 (2005).
[12] J. C. Crocker and D. G. Grier, J. Colloid Interface Sci. **179**, 298 (1996).
[13] S.-H. Lee and D. G. Grier, Phys. Rev. Lett. **96**, 190601 (2006).
[14] C. Pozrikidis, *Boundary Integral and Singularity Methods for Linearized Viscous Flow* (Cambridge University Press, New York, 1992).
[15] C. Lutz, M. Kollmann, and C. Bechinger, Phys. Rev. Lett. **93**, 026001 (2004).
[16] C. Lutz, M. Kollmann, P. Leiderer, and C. Bechinger, J. Phys.: Condens. Matter **16**, S4075 (2004).
[17] J. P. Gollub and S. V. Benson, Phys. Rev. Lett. **41**, 948 (1978).
[18] G. M. Zaslavsky, Phys. Lett. **69**, 145 (1978).
[19] G. M. Zaslavsky, Phys. Rep. **371**, 461 (2002).
[20] E. L. Rempel, A. C. L. Chian, A. J. Preto, and S. Stephany, Nonlinear Processes Geophys. **11**, 691 (2004).
[21] L. F. Burlaga and A. F. Vinas, Physica A **356**, 375 (2005).
[22] J. Jimenez and M. P. Simens, J. Fluid Mech. **435**, 81 (2001).
[23] J. P. Crutchfield and B. A. Huberman, Phys. Lett. **77**, 407 (1980).
[24] Q. D. Wang and L. S. Young, Commun. Math. Phys. **225**, 275 (2002); **218**, 1 (2001).
[25] G. M. Zaslavsky, M. Edelman, H. Weitzner, B. Carreras, G. McKee, R. Bravenec, and R. Fonck, Phys. Plasmas **7**, 3691 (2000).
[26] D. Sornette, Physica A **250**, 295 (1998).